Draft version November 23, 2022
Typeset using LaTeX **twocolumn** style in AASTeX631

Daksha: On Alert for High Energy Transients

Varun Bhalerao,[1] Santosh Vadawale,[2] Shriharsh Tendulkar,[3] Dipankar Bhattacharya,[4] Vikram Rana,[5] Hitesh Kumar L. Adalja,[2] Hrishikesh Belatikar,[6] Mahesh Bhaganagare,[6] Gulab Dewangan,[7] Abhijeet Ghodgaonkar,[1] Shiv Kumar Goyal,[2] Suresh Gunasekaran,[8] Guruprasad P J,[8] Jayprakash G. Koyande,[3] Salil Kulkarni,[9] APK Kutty,[3] Tinkal Ladiya,[2] Deepak Marla,[9] Sujay Mate,[3] N.P.S. Mithun,[2] Rakesh Mote,[9] Sanjoli Narang,[6] Ayush Nema,[3] Sudhanshu Nimbalkar,[6] Archana Pai,[1] Sourav Palit,[10] Arpit Patel,[2] Jinaykumar Patel,[11,8] Priya Pradeep,[12] Prabhu Ramachandran,[8] B.S. Bharath Saiguhan,[2] Divita Saraogi,[1] Disha Sawant,[1,13] M. Shanmugam,[2] Piyush Sharma,[2] Amit Shetye,[6] Shreeya Singh,[14] Nishant Singh,[2] Akshat Singhal,[1] S. Sreekumar,[12] Srividhya Sridhar,[8,15] Rahul Srinivasan,[16,17,1] Siddharth Tallur,[6] Neeraj K. Tiwari,[2] Amrutha Lakshmi Vadladi,[9] C. S. Vaishnava,[2] Sandeep Vishwakarma,[3] and Gaurav Waratkar[1]

[1]*Department of Physics, IIT Bombay, Powai, Mumbai 400076, India*
[2]*Physical Research Laboratory, Navrangpura, Ahmedabad 380009, India*
[3]*Department of Astronomy and Astrophysics, Tata Institute of Fundamental Research, Mumbai, 400005, India*
[4]*Ashoka University, Department of Physics, Sonepat, Haryana 131029, India*
[5]*Raman Research Institute, C. V. Raman Avenue, Sadashivanagar, Bengaluru 560080, India*
[6]*Department of Electrical Engineering, IIT Bombay, Powai, Mumbai 400076, India*
[7]*Inter-University Center for Astronomy and Astrophysics, Pune, Maharashtra-411007, India*
[8]*Department of Aerospace Engineering, IIT Bombay, Powai, Mumbai 400076, India*
[9]*Department of Mechanical Engineering, IIT Bombay, Powai, Mumbai 400076, India*
[10]*Indian Center for Space Physics, Kolkata, West Bengal 700084*
[11]*Department of Mechanical and Aerospace Engineering, The University of Texas at Arlington, Arlington, TX 76019, USA*
[12]*Vikram Sarabhai Space Centre, Kochuveli, Thiruvananthapuram, 695022, India*
[13]*Pune Knowledge Cluster, Pune 411007, India*
[14]*Department of Chemical Engineering, IIT Bombay, Powai, Mumbai 400076, India*
[15]*Department of Aerospace, University of Illinois Urbana-Champaign - 61801, US.*
[16]*Université Côte d'Azur, Observatoire de la Côte d'Azur, CNRS, Laboratoire Lagrange, Bd de l'Observatoire, CS 34229, 06304 Nice cedex 4, France*
[17]*Artemis, Université Côte d'Azur, Observatoire de la Côte d'Azur, CNRS, F-06304 Nice, France*

ABSTRACT

We present *Daksha*, a proposed high energy transients mission for the study of electromagnetic counterparts of gravitational wave sources, and gamma ray bursts. *Daksha* will comprise of two satellites in low earth equatorial orbits, on opposite sides of earth. Each satellite will carry three types of detectors to cover the entire sky in an energy range from 1 keV to > 1 MeV. Any transients detected on-board will be announced publicly within minutes of discovery. All photon data will be downloaded in ground station passes to obtain source positions, spectra, and light curves. In addition, *Daksha* will address a wide range of science cases including monitoring X-ray pulsars, studies of magnetars, solar flares, searches for fast radio burst counterparts, routine monitoring of bright persistent high energy sources, terrestrial gamma-ray flashes, and probing primordial black hole abundances through lensing. In this paper, we discuss the technical capabilities of *Daksha*, while the detailed science case is discussed in a separate paper.

Keywords: space vehicles: instruments — instrumentation: detectors

1. INTRODUCTION

Daksha is a proposed high-energy transients mission comprising of two satellites monitoring the entire sky in the 1—1000 keV range. The primary science goals of *Daksha* are the study of electromagnetic counterparts to gravitational wave sources, and prompt emission gamma ray bursts (GRBs). In addition, *Daksha* will also study

X-ray pulsars, create a high-energy all-sky map with Compton imaging, and detect X-ray polarization from transients and pulsars.

The key science goal driving the *Daksha* mission is the detection of high energy counterparts to gravitational wave events. Multi-messenger astrophysics has received a great boost in the last decade with the joint detection of gravitational waves (GW) and electromagnetic (EM) radiation from a binary neutron star merger, GW170817 (LIGO Scientific Collaboration et al. 2017; Abbott et al. 2017). This was a treasure–trove of physics — in addition to being the first direct proof of a link between short GRBs and binary neutron star (BNS) mergers, it provided insights into r-process nucleosynthesis (Watson et al. 2019; Kasliwal et al. 2019), yielded an independent measurement of H_0 (LIGO Scientific Collaboration et al. 2021), measurements of equation of state (De et al. 2018). However, no EM counterparts could be found for subsequent binary neutron star mergers detected by the advanced GW networks (see for instance Hosseinzadeh et al. 2019; Coughlin et al. 2019). This was not very surprising: scaling the event flux from GW170817 to distances of the other events puts it beyond the sensitivity of most satellites. Indeed, if the gamma ray emission from GW170817 was just 30% fainter, it would have been missed by current satellites (see for instance Goldstein et al. 2017). The EM sensitivity to such events is already lagging behind the GW sensitivity to such mergers, despite the latter field being only a few years old. *Daksha* attempts to bridge this gap by drastically improving the sensitivity for high energy transients over current missions.

A closely related field is the study of long and short gamma ray bursts. Great progress has been made in this field, led by missions like BATSE, Swift (Gehrels et al. 2004) and Fermi (Meegan et al. 2009). More recently, *AstroSat* CZTI (Bhalerao et al. 2017a) and POLAR (Produit et al. 2005) have characterized the polarization of GRBs. *Daksha* will detect a large number of gamma ray bursts per year, making significant strides in studies of soft prompt emission, high redshift GRBs, and GRB polarization. In addition two these two primary science goals, *Daksha* data will give insights into a wide variety of science: including high energy emission in FRBs, studies of accreting pulsars, Soft Gamma Repeaters, monitoring bright sources with Earth Occultation, solar studies, Terrestrial Gamma-ray Flashes (TGFs), and probing primordial black holes with gravitational lensing. In this paper, we describe the design and capabilities of *Daksha*, and defer a detailed discussion of the science case to Bhalerao et al., (2022) (hereafter Paper II).

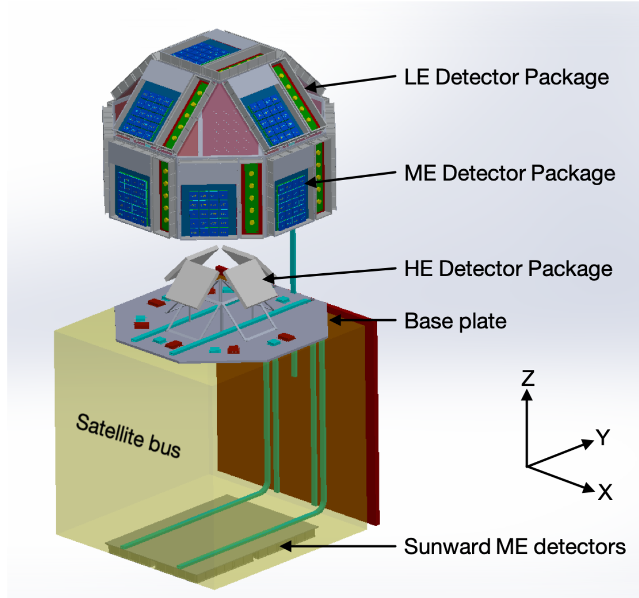

Figure 1. Overall design of a *Daksha* satellite. The dome-shaped payload has 13 surfaces, each carrying Low-energy (LE) and Medium-energy (ME) detector packages. Four ME detector packages are mounted under the satellite bus, and always point directly to the sun. Four High-energy (HE) detector packages are mounted inside the dome, along with processing electronics.

2. DAKSHA

The science goals for *Daksha* can be mapped to three key technical requirements: high sensitivity, continuous all-sky coverage, broadband response. In order to achieve these goals, *Daksha* has been designed as two identical satellites in low-earth orbit (LEO), on opposite sides of the Earth. We aim for an *AstroSat*-like near-equatorial orbit with an inclination of 6° and an altitude of $\sim$ 650 km (Singh et al. 2014). The broadband response will be attained by using three types of detectors: Silicon Drift Detectors (SDDs), Cadmium Zinc Telluride detectors (CZT), and NaI (Tl) scintillators for Low, Medium and High energies respectively. These are discussed in more detail in §3.

The main payload shape is a partial rhombicuboctahedron[1] with 13 square and 4 triangular surfaces, approximating a hemisphere as shown in Fig 1. Medium and low energy detector packages are mounted on each square surface. The "base plate" is a flat octagon that carries the high energy detectors, and will be mounted on the satellite bus. Four medium energy detector packages are mounted under the bus.

[1] A rhombicuboctahedron is a solid with eighteen square and eight equilateral triangular surfaces.

The satellite will be oriented such that the dome-shaped payload always points away from the sun, and the four medium energy detector packages under the satellite bus will always point at the sun. We refer to the "anti-sun" direction (upwards in Fig 1) as the boresight. The symmetrical design of the payload ensures good azimuthal uniformity (around the boresight) in the effective area (§4).

3. SPECTRAL RANGE

Daksha will attain broadband spectral sensitivity from 1 keV to >1 MeV by using SDDs for the low energy band (LE; 1–30 keV), CZT detectors for the medium energy band (ME; 20–200 keV), and NaI Scintillator with Silicon Photomultipliers (NaI + SiPM) for the high energy band (HE; 100–1000+ keV). Detectors were selected on the basis of their characteristics like the active area, noise properties, sensitivity, and energy range. All these detectors have been validated for space use in environmental tests or in previous space missions.

3.1. *Medium Energy*

The workhorses for *Daksha* are sensitive pixelated CZT detectors. We use 5 mm thick detectors manufactured by GE Medical, sensitive to an energy range from 20 keV to 200 keV with an energy resolution of 12% at 60 keV. Each 3.9 cm × 3.9 cm detector is divided into a 16×16 pixel array, and integrated electronics provide a digital readout. Detector operating temperatures will be attained using passive cooling with a radiator plate. These detectors have been used before in several space experiments including RT2 (Nandi et al. 2009), High Energy X-ray Spectrometer on Chandrayaan-1 (Vadawale et al. 2009), and CZT Imager on *AstroSat* (Rao et al. 2017; Bhalerao et al. 2017a) where they have proven to be space-worthy and highly effective for this energy range.

Twenty CZT detectors will assembled into a Medium Energy Package (MEP; Figure 2) that contains necessary electronics and a heat sink to cool the detectors. The number of detectors in each package determines the sensitivity of *Daksha*, and is discussed in §5. Thirteen such identical packages will be placed on the thirteen square surfaces on the dome of *Daksha*. Hence, four MEPs will be mounted on the sunward side of the satellite in order to complete the coverage of the entire sky. This number is chosen to obtain similar effective area as the dome-shaped payload. While the sun is very bright in soft X-rays, solar flux is considerably lower in the ME detector energy range (Hannah et al. 2010) — thus these detectors do not risk being saturated in regular observations.

Figure 2. Laboratory model of a *Daksha* ME Package, with all detectors mounted. External connections are not shown in this photograph. Each *Daksha* will have 17 such MEPs.

Photon events will be time-tagged with ∼ microsecond accuracy. Compton scattering can create double events within the detector, which can be used to study polarization of sources as has been demonstrated with *AstroSat* CZTI (Chattopadhyay et al. 2022; Chattopadhyay et al. 2019; Vadawale et al. 2018, 2015). We have undertaken detailed simulations of the polarization sensitivity, and the results will be presented in Bala et al., in prep.

3.2. *Low Energy*

Daksha Low Energy (LE) detectors have to provide sensitivity down to 1 keV, while overlapping with the ME detector energy range at the higher side. In our baseline design, the low energy coverage will be provided by SDDs with an active thickness of 450 μm to cover the low energy range from 1–30 keV. We use SDD modules with 1.5 cm^2 collecting area, and a thin Beryllium window to block lower energy photons. Low electronic noise is achieved by means of a built-in thermo-electric cooler. These devices have an energy resolution of ∼2.5% (at 5.9 keV) and a timing resolution of 10 μs. These modules have been used in the APXS and XSM payloads on Chandrayaan-2 (Shanmugam et al. 2020; Vadawale et al. 2014).

A standard Low Energy Package (LEP) will consist of five Low Energy SDDs, their electronics, and active cooling systems. One LEP will be mounted next to the MEP on each of the thirteen surfaces on the top dome. As the bright sun can saturate LE detectors, no LEPs are mounted on the sunward side of the satellite.

3.3. *High Energy*

At high energies, the coverage of CZT detectors is complemented by Thallium activated Sodium Iodide scintillators, NaI (Tl). Each high energy detector package (HEP) consists of a 20 cm × 20 cm × 2 cm NaI(Tl) crystal, sensitive to photons from ∼100 keV to >1 MeV. The detector works on a sparse array of Si-PM with uniform spatial sensitivity operating on low voltage (∼40 V). This arrangement ensures uniform light collection, and also gives high position sensitivity with spatial resolution of ∼1 cm. Photons will be time-tagged with microsecond accuracy. The dome, covered with LE and ME packages, gets progressively transparent at energies $\gtrsim$ 150 keV. Hence, we place the HE scintillators inside the dome on the base plate. We opt for four HE detector packages mounted parallel to the four inclined square faces of the dome. This enables us to detect Compton pairs of photons scattered from one of the ME detectors and absorbed in the HE detector, which will help in localizing transient sources and creating an all-sky Compton map of persistent sources.

All the power electronics and processing electronics will be mounted on the base plate.

4. ALL-SKY COVERAGE

The quasi-hemispherical design of the payload naturally results in nearly uniform sensitivity over half of the sky. This design also gives good angular resolution for source localization, discussed in §6. The MEPs mounted under the spacecraft bus extend this sensitivity to the rest of the sky as well, though localization abilities become poorer for sources closer to the satellite $-Z$ axis. For a satellite in low-earth orbit at an altitude of ∼ 650 km, about 29% of the sky is occulted by the Earth. Further, the satellite will spend an average of 24% of its time in the South Atlantic Anomaly (SAA) region where the high charged particle concentration poses a risk to high voltage electronics and detectors have to be deactivated. As a result, the time-averaged sky coverage of a single satellite in equatorial low earth orbit is limited to about 56%.

To overcome this limitation, the *Daksha* mission will will deploy two satellites on opposite sides of the Earth. In this configuration we get 100% sky coverage when neither of the satellites is in the SAA. When either one of the satellites is in SAA, we get 71% coverage as before. Hence, the total sky coverage of the twin-satellite *Daksha* mission is ∼ 86%.

5. SENSITIVITY

A key requirement for *Daksha* is to have significantly higher sensitivity for short bursts, as compared to existing missions. The on-axis effective area of each MEP is 304 cm^2 on each surface. Considering projection effects over the entire visible sky, the median effective area for

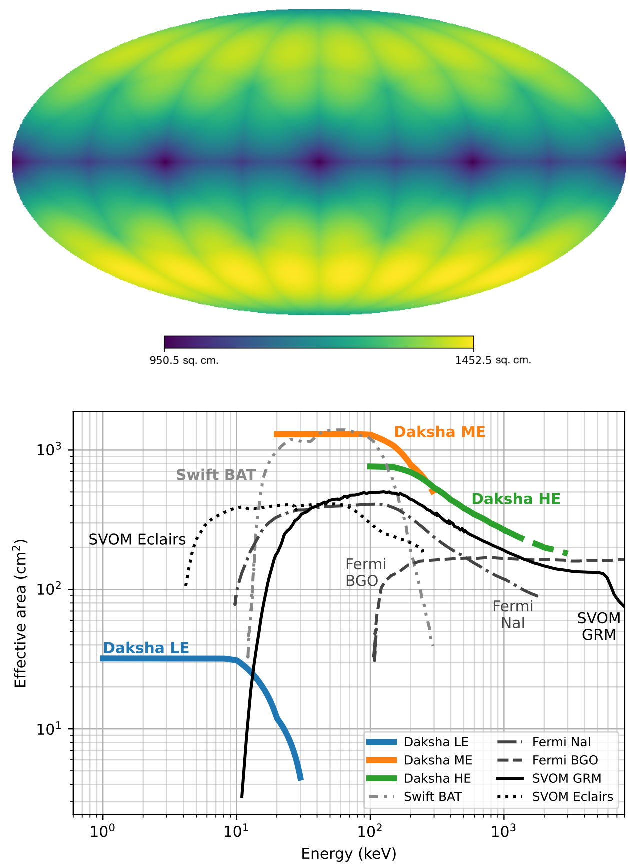

Figure 3. *Top:* Effective area as a function of position, in satellite coordinates. The satellite boresight is at the top, and the sun will always be at the bottom. About 29% of the sky will be occulted by the Earth at any given instant. *Bottom:* Effective area with respect to detector's energy coverage. Effective areas of *Swift*-BAT (imaging effective area, with mask) and both NaI and BGO detectors of *Fermi*-GBM are shown for comparison. These areas were adapted from (Luo et al. 2020). The NaI effective area is the averaged over the unocculted sky.

Daksha ME detectors is 1316 cm^2 at 100 keV (ignoring effects of Earth occultation; Figure 3). Accounting for the varying satellite-Earth vector through the orbit, the median un-occulted effective area is 1310 cm^2. This is significantly higher than the 126 cm^2 on-axis effective area for individual NaI modules on *Fermi* GBM (Meegan et al. 2009), which has a similar orbit and also covers the entire non-occulted sky. Our effective area is comparable to the masked effective area of the Burst Alert Telescope (BAT) on the Neil Gehrels *Swift* Observatory (Gehrels et al. 2004; Barthelmy et al. 2005), though *Swift*-BAT can observe only about 11% of the sky as opposed to 71% for each *Daksha* satellite. The effective area gradually tapers off above 100 keV.

A transient located anywhere in the sky will be incident on 4-10 ME packages. Out of these, several will have glancing incidence angles such that the projected area is very small. Ignoring the MEPs with projected area < 40 cm^2, the median number of packages that detect any source is 7. In practice, such a cut does not drastically affect the total effective area: after applying this filter, the all-sky median effective area becomes 1296 cm^2. To calculate the sensitivity, we assume that the background count rate is same for all ME packages. Thus, we have a source signal corresponding to the median effective area ($\sim$ 1300 cm^2, and background noise corresponding to surfaces on which the transient is incident (typically 7).

The HEPs give a smooth continuation of the MEP effective area at higher energies, extending beyond 1 MeV. The median all-sky effective area for HEPs is 762 cm^2. This number will decrease when a detailed model of the satellite bus is included in the calculation.

The LEPs have a median effective area of 32.0 cm^2 in the anti-sun direction, accounting for projection effects. The effective area slowly drops off in the sunward direction, and the all-sky median effective area is 26.0 cm^2.

The flux sensitivity depends on the source spectrum and background rates. We estimate the background with a GEANT4 simulation that includes the cosmic diffuse X-ray background, particle-induced backgrounds, and albedo components. We also add a component for electronic noise, estimated from the CZTI instrument on *AstroSat* (Bhalerao et al. 2017a). By considering all components, we estimate the net background count rate to be about 10 counts cm^2 s^{-1}.

To be conservative and avoid false negatives, we select a detection threshold as a signal-to-noise ratio of 5, for a burst of 1 second duration. Assuming a typical GRB-like Band spectrum, the faintest sources that *Daksha* can detect have a flux of 4×10^{-8} erg cm^{-2} s^{-1} (1 s, 5-σ). The numbers of course depend on burst duration and the sensitivity threshold. For instance, the 3-σ limit for a 20 s burst is $0.5{\times}10^{-8}$ erg cm^{-2} s^{-1}. Adopting a more conservative threshold for short bursts, the 7-σ sensitivity for 1 s bursts is $5.6{\times}10^{-8}$ erg cm^{-2} s^{-1}.

In Table 1, we compare the sensitivity of *Daksha* with various other missions, scaled to the same detection criteria. We calculate the distance to which the missions would be sensitive to GW170817, assuming a "Comptonized" spectral model with a photon power-law index $\alpha = -0.62$, an exponential cut-off at $E_p = 185$ keV, duration $\Delta t = 0.576$ s (Goldstein et al. 2017). The luminosity is calculated to match the observed Fermi flux of $3.1{\times}10^{-7}$ erg cm^{-2} s^{-1} in the 10–1000 keV band. The "range" column of the table shows the distance to which such a source could be detected by each mission. The relevant figure of merit is now the total volume probed by each mission, derived from the range and the field of view. We can see that *Daksha* probes a significantly higher volume than any other mission.

6. LOCALIZATION

The focus of the *Daksha* mission is to detect transients, and we trade off angular resolution for all-sky coverage. Based on our calculated background rates, we find that a short GRB ($T_{90} = 1$ s) with a fluence of 10^{-7} erg cm^{-2} can be localized with an accuracy of 10°. The localization accuracy depends on the source spectrum, the T_{90}, and also on the position of the transient in the satellite frame — with worse angular resolution on sunward side of the satellite. For a given fluence, a longer GRB will be localized more poorly due to the higher number of background counts in that duration. Angular resolution is approximately inversely proportional to flux, such that a 1 s GRB with flux 10^{-6} erg cm^{-2} s^{-1} can be localized to an accuracy of $\approx 1^\circ$. At this flux level, the background contribution becomes comparable to the number of source photons in the ME detectors.

For transients detected by both satellites, the location can be improved by joint triangulation of the source. On-board clocks on *Daksha* will have an absolute timing accuracy of at least 1 ms. For transients with sufficiently high fluence, joint analysis of data from both satellites (including projection effects and light-travel delay) can be used to obtain source positions with 1–2° accuracy. *Daksha* could also be used along with other satellites analogous to the Interplanetary Network (IPN[2]), to obtain more precise transient locations.

7. ALERTS AND DATA

Daksha satellites will have robust on-board processing capabilities to detect transients. For each detected transient, on-board software will calculate the source position, spectrum, and T_{90}. It will also create a light curve in multiple bands, and low-resolution spectra to create a $\sim$ 2 kB data package. Our mission requirements are to be able to download this information within 1 minute of transient detection, for >95% of the orbit. Transient detections will be announced immediately through standard channels like the General Coordinates Network[3] (Barthelmy 2000; Barthelmy et al. 2022).

[2] http://www.ssl.berkeley.edu/ipn3/

[3] https://gcn.gsfc.nasa.gov/, formerly GRB Coordinates Network.

Table 1. Comparison of key parameters of GRB missions.

Mission name	Energy range (keV)	Effective area (cm^2)	FoV Sky fraction	FoV (sr)	Range Mpc	Volume Mpc^3	Sensitivity (1-s, 5σ) erg cm^{-2} s^{-1}	Sensitivity (1-s, 5σ) ph cm^{-2} s^{-1}	Reference
Daksha (single)	20–200	1300	0.7	8.8	76	1.27×10^6	4×10^{-8}	0.6	This work
Daksha (two)	20–200	1700	1	12.6	76	1.81×10^6	4×10^{-8}	0.6	This work
Swift-BAT	15–150	1400	0.11	1.4	67	0.14×10^6	3×10^{-8}	0.5	(a)
Fermi-GBM	50–300	420	0.7	8.8	49	0.35×10^6	20×10^{-8}	0.5	(b)
GECAM-B	6–5000	480	0.7	8.8	65	0.81×10^6	9×10^{-8}	—	(c)
SVOM/ECLAIRs	4–150	400	0.16	2	70	0.23×10^6	4×10^{-8}	0.8	(d)
THESEUS/XGIS	2–30	500	0.16	2	45	0.06×10^6	1.7×10^{-8}	—	(e)
THESEUS/XGIS	30–150	500	0.16	2	58	0.12×10^6	5×10^{-8}	—	(e)
THESEUS/XGIS	150–1000	1000	0.5	6.2	20	0.02×10^6	45×10^{-8}	—	(e)

Note—Sensitivity numbers are scaled to 5-σ threshold for a 1 s transient. The sensitivity numbers should be compared with caution: for instance for power-law spectrum with photon index $\alpha = -1$, the *Swift*-BAT 15–150 keV sensitivity limit of 3×10^{-8} erg cm^{-2} s^{-1} is equivalent to the *Daksha* 20–200 keV sensitivity limit 4×10^{-8} erg cm^{-2} s^{-1}. The Field of View is the peak FoV, and does not include any temporal downtime corrections.

"Range" and "Volume" are calculated for GW170817 as discussed in the text. *Swift*-BAT range is taken from Tohuvavohu et al. (2020), our estimate was higher (79 Mpc), the difference likely comes from not accounting for reduced number of detectors currently operational. *Fermi*-GBM calculated range is consistent with Tohuvavohu et al. (2020); Goldstein et al. (2017). Range for other instruments is calculated from the sensitivity numbers used in this table.

The sky coverage is instantaneous. This table does not correct for any instrument downtime from SAA passages or any other causes.

References—(a) Lien et al. (2014), https://swift.gsfc.nasa.gov/about_swift/bat_desc.html, https://swift.gsfc.nasa.gov/analysis/bat_digest.html, (b) von Kienlin et al. (2020); Poolakkil et al. (2021), https://fermi.gsfc.nasa.gov/science/instruments/table1-2.html, (c) Zheng (2019); Zhang et al. (2019), (d) Lacombe et al. (2019), (e) Labanti et al. (2021) .

All time-tagged event data from all detectors will be stored on-board, and will be downlinked on every ground station pass. Offline analysis will account for secondary effects like scattering of photons within the satellite and the Earth albedo, to produce more accurate localizations and spectra. All data and data products will be made public after a limited proprietary period, using standard FTOOLs-compatible FITS formats (Wells et al. 1981; Blackburn 1995).

8. INTERNATIONAL SCENARIO

The *Daksha* mission has excellent synergy with the rapidly growing field of time–domain astrophysics. *Daksha* will search for counterparts to events from the advanced gravitational-wave detector network of LIGO (LIGO Scientific Collaboration et al. 2015), Virgo (Acernese et al. 2015), KAGRA (KAGRA Collaboration et al. 2020), and LIGO-India (Iyer et al. 2011; Saleem et al. 2022). *Daksha* transients can be triggers to optical synoptic and survey telescopes like the Vera Rubin Observatory (LSST Science Collaboration et al. 2009) and the Zwicky Transient Facility (ZTF; Bellm 2014). Conversely, *Daksha* data can also be searched for high energy bursts associated with rapidly evolving transients discovered in such surveys as has often been done with *AstroSat* and other missions (See for instance Bhalerao et al. 2017b; Andreoni et al. 2021). Similar synergy will also exist with radio facilities like the Square Kilometer Array (Dewdney et al. 2009), Australian Square Kilometer Array Pathfinder (Johnston et al. 2007), Low-Frequency Array (LOFAR; van Haarlem et al. 2013), upgraded Giant Metrewave Radio Telescope (uGMRT; Gupta et al. 2017), etc.

The current key spacecraft for high energy transient studies — the Neil Gehrels Swift Observatory (Gehrels et al. 2004) and *Fermi* (Meegan et al. 2009) — are over fifteen years old. Indeed, the Astro2020 decadal survey concluded that, "In space, the highest-priority sustaining activity is a space-based time-domain and multi-messenger program of small and medium-scale missions" (National Academies of Sciences Engineering and Medicine 2021). A recent mission in the field is *GECAM* (Gravitational wave high-energy Electromagnetic Counterpart All-sky Monitor; Zhang et al. 2019), launched in late 2020. While the mission concept is very similar to *Daksha*, *GECAM* is based completely on scintillator-based detectors, and has lower sensitivity (Zheng 2019). Another upcoming high energy transient mission is *SVOM* (Space Variable Objects Monitor; Cordier et al. 2015) is a multi-wavelength mission with capabilities to detect GRBs. The CZT-based ECLAIRS instrument (Godet et al. 2014) is a coded mask imager with field of view of ~ 2 steradians, and active area of 1024 cm^2 (40% mask transparency). It is complemented at higher energies by GRM, covering the same part of the sky with sensitivity similar to *Fermi*-GBM Wei et al. (2016). Several teams have also proposed smaller satellites like BurstCube (Racusin et al. 2017), HER-

MES (Fuschino et al. 2019), BlackCAT (Chattopadhyay et al. 2018) etc, with limited effective areas. With significantly higher sensitivity and grasp compared to all these, *Daksha* will revolutionize our understanding of highly energetic transients.

9. SUMMARY AND CURRENT STATUS

Daksha is an ambitious high energy transients mission designed to have high sensitivity, all-sky coverage, and broadband spectral response. The science of *Daksha* is discussed in detail in Paper II, we only list the highlights here. *Daksha* will detect high-energy emission from about 3–12 off–axis neutron star bursts each year, depending on assumed model. In addition, *Daksha* can discovery up to 7 more each year which are just sub-threshold for the GW detector networks, but maybe recovered given the confident electromagnetic trigger. *Daksha* will detect about 500 long GRBs and 50 short GRBs each year and provide time-tagged event data from 1 keV to > 1 MeV for each of these events. *Daksha* will be the first all-sky monitor to obtain soft X-ray spectra of these transients. Furthermore, *Daksha* will address a wide range of science cases including studying GRB hard X-ray polarisation, monitoring X-ray pulsars, studies of magnetars, solar flares, searches for fast radio burst counterparts, routine monitoring of bright persistent high energy sources, terrestrial gamma-ray flashes, and probing primordial black hole abundances through lensing.

Daksha was proposed in response to the Indian Space Research Organisation's Announcement of Opportunity (AO) for Astronomy missions in 2018. The proposal was shortlisted for further studies, and was awarded seed funding by the Space Science Program Office for demonstration of a proof-of-concept. The team has completed the construction and testing of a laboratory model of the Medium Energy detector Package, as required. *Daksha* builds heavily on the legacy of various Indian space science missions, giving a high technology readiness level to all subsystems. The mission will be reviewed for full approval, after which we target a development timeline of three years to launch.

We thank the Space Program Office (SPO) of the Indian Space Research Organisation for its Announcement of Opportunity for space astrophysics missions, under which *Daksha* was proposed. Development of the *Daksha* MEP laboratory model was started with funding support from SPO. We thank the administrative and support staff at all partner institutes for their help in all *Daksha*-related matters.

DS was supported under the CEFIPRA Grant No. IFC/5404-1. AP acknowledges the SERB Matrics grant MTR/2019/001096 and SERB-Power-fellowship grant SPF/2021/000036 of Department of Science and Technology, India for support.

Software: Numpy (van der Walt et al. 2011), Matplotlib (Hunter 2007), Astropy (Robitaille et al. 2013, http://www.astropy.org), HealPIX (Gorski et al. 2005), Healpy (https://healpy.readthedocs.org/), Ephem (https://pypi.python.org/pypi/pyephem/).

REFERENCES

Abbott, B., Abbott, R., Abbott, T., et al. 2017, ApJL, 848, L12, doi: 10.3847/2041-8213/aa91c9

Acernese, F., Agathos, M., Agatsuma, K., et al. 2015, Classical and Quantum Gravity, 32, 024001, doi: 10.1088/0264-9381/32/2/024001

Andreoni, I., Coughlin, M. W., Kool, E. C., et al. 2021, ApJ, 918, 63, doi: 10.3847/1538-4357/ac0bc7

Barthelmy, S., Burns, E., Dutko, D., et al. 2022, GRB Coordinates Network, 32419, 1

Barthelmy, S. D. 2000, in AIPC, Vol. 526 (AIP Publishing), 731–735, doi: 10.1063/1.1361631

Barthelmy, S. D., Barbier, L. M., Cummings, J. R., et al. 2005, Space Science Reviews, Volume 120, Issue 3-4, pp. 143-164, 120, 143, doi: 10.1007/s11214-005-5096-3

Bellm, E. 2014, in The Third Hot-wiring the Transient Universe Workshop, ed. P. R. Wozniak, M. J. Graham, A. A. Mahabal, & R. Seaman, 27–33. https://arxiv.org/abs/1410.8185

Bhalerao, V., Bhattacharya, D., Vibhute, A., et al. 2017a, Journal of Astrophysics and Astronomy, 38, 31, doi: 10.1007/s12036-017-9447-8

Bhalerao, V., Kasliwal, M., Bhattacharya, D., et al. 2017b, Astrophysical Journal, 845, doi: 10.3847/1538-4357/aa81d2

Blackburn, J. K. 1995, Astronomical Data Analysis Software and Systems IV, 77. http://adsabs.harvard.edu/abs/1995ASPC...77..367B

Chattopadhyay, T., Falcon, A. D., Burrows, D. N., Fox, D. B., & Palmer, D. 2018, in Society of Photo-Optical Instrumentation Engineers (SPIE) Conference Series, Vol. 10699, Space Telescopes and Instrumentation 2018: Ultraviolet to Gamma Ray, ed. J.-W. A. den Herder, S. Nikzad, & K. Nakazawa, 106995S, doi: 10.1117/12.2314274

Chattopadhyay, T., Vadawale, S. V., Aarthy, E., et al. 2019, \apj, 884, 123, doi: 10.3847/1538-4357/ab40b7

Chattopadhyay, T., Gupta, S., Iyyani, S., et al. 2022, ApJ, 936, 12, doi: 10.3847/1538-4357/ac82ef

Cordier, B., Wei, J., Atteia, J. L., et al. 2015, arXiv e-prints, 13. https://arxiv.org/abs/1512.03323

Coughlin, M. W., Ahumada, T., Anand, S., et al. 2019, The Astrophysical Journal Letters, 885, L19. https://arxiv.org/abs/1907.12645

De, S., Finstad, D., Lattimer, J. M., et al. 2018, PhRvL, 121, 091102, doi: 10.1103/PhysRevLett.121.091102

Dewdney, P. E., Hall, P. J., Schilizzi, R. T., & Lazio, T. J. L. W. 2009, IEEE Proceedings, 97, 1482, doi: 10.1109/JPROC.2009.2021005

Fuschino, F., Campana, R., Labanti, C., et al. 2019, Nuclear Instruments and Methods in Physics Research A, 936, 199, doi: 10.1016/j.nima.2018.11.072

Gehrels, N., Chincarini, G., Giommi, P., et al. 2004, The Astrophysical Journal, 611, 1005, doi: 10.1086/422091

Godet, O., Nasser, G., Atteia, J. ., et al. 2014, in Society of Photo-Optical Instrumentation Engineers (SPIE) Conference Series, Vol. 9144, Space Telescopes and Instrumentation 2014: Ultraviolet to Gamma Ray, ed. T. Takahashi, J.-W. A. den Herder, & M. Bautz, 914424, doi: 10.1117/12.2055507

Goldstein, A., Veres, P., Burns, E., et al. 2017, The Astrophysical Journal, 848, L14, doi: 10.3847/2041-8213/aa8f41

Gorski, K. M., Hivon, E., Banday, A. J., et al. 2005, The Astrophysical Journal, 622, 759, doi: 10.1086/427976

Gupta, Y., Ajithkumar, B., Kale, H. S., et al. 2017, Current Science, 113, 707, doi: 10.18520/cs/v113/i04/707-714

Hannah, I. G., Hudson, H. S., Hurford, G. J., & Lin, R. P. 2010, The Astrophysical Journal, 724, 487, doi: 10.1088/0004-637x/724/1/487

Hosseinzadeh, G., Cowperthwaite, P. S., Gomez, S., et al. 2019, The Astrophysical Journal, 880, L4, doi: 10.3847/2041-8213/ab271c

Hunter, J. D. 2007, Computing in Science & Engineering, 9, 90, doi: 10.1109/MCSE.2007.55

Iyer, B., et al. 2011. https://dcc.ligo.org/ligo-M1100296/public

Johnston, S., Bailes, M., Bartel, N., et al. 2007, PASA, 24, 174, doi: 10.1071/AS07033

KAGRA Collaboration, Akutsu, T., Ando, M., et al. 2020, arXiv e-prints, arXiv:2008.02921. https://arxiv.org/abs/2008.02921

Kasliwal, M. M., Kasen, D., Lau, R. M., et al. 2019, Monthly Notices of the Royal Astronomical Society: Letters, L14, doi: 10.1093/mnrasl/slz007

Labanti, C., Amati, L., Frontera, F., et al. 2021, arXiv e-prints, arXiv:2102.08701. https://arxiv.org/abs/2102.08701

Lacombe, K., Amoros, C., Atteia, J.-L., et al. 2019, Experimental Astronomy, 47, 245, doi: 10.1007/s10686-019-09626-y

Lien, A., Sakamoto, T., Barthelmy, S. D., et al. 2014, in Proceedings of Science, Vol. 829 (Proceedings of Science (PoS)), 7, doi: 10.3847/0004-637x/829/1/7

LIGO Scientific Collaboration, Virgo Collaboration, Fermi Gamma-Ray Burst Monitor, & INTEGRAL. 2017, The Astrophysical Journal, 848, 13, doi: 10.3847/2041-8213/aa920c

LIGO Scientific Collaboration, Aasi, J., Abbott, B. P., et al. 2015, Classical and Quantum Gravity, 32, 074001, doi: 10.1088/0264-9381/32/7/074001

LIGO Scientific Collaboration, Virgo Collaboration, Abbott, B. P., et al. 2021, ApJ, 909, 218, doi: 10.3847/1538-4357/abdcb7

LSST Science Collaboration, Abell, P. A., Allison, J., et al. 2009, eprint arXiv:0912.0201. http://adsabs.harvard.edu/abs/2009arXiv0912.0201Lhttp://www.lsst.org/lsst/scibook

Luo, Q., Liao, J.-Y., Li, X.-F., et al. 2020, Journal of High Energy Astrophysics, 27, 1, doi: 10.1016/j.jheap.2020.04.004

Meegan, C., Lichti, G., Bhat, P. N., et al. 2009, The Astrophysical Journal, 702, 791, doi: 10.1088/0004-637X/702/1/791

Nandi, A., Rao, A. R., Chakrabarti, S. K., et al. 2009, arXiv e-prints, arXiv:0912.4126. https://arxiv.org/abs/0912.4126

National Academies of Sciences Engineering and Medicine. 2021, Pathways to Discovery in Astronomy and Astrophysics for the 2020s (Washington, DC: The National Academies Press), doi: 10.17226/26141

Poolakkil, S., Preece, R., Fletcher, C., et al. 2021, ApJ, 913, 60, doi: 10.3847/1538-4357/abf24d

Produit, N., Barao, F., Deluit, S., et al. 2005, Nuclear Instruments and Methods in Physics Research A, 550, 616, doi: 10.1016/j.nima.2005.05.066

Racusin, J., Perkins, J. S., Briggs, M. S., et al. 2017, arXiv e-prints, arXiv:1708.09292. https://arxiv.org/abs/1708.09292

Rao, A. R., Bhattacharya, D., Bhalerao, V. B., Vadawale, S. V., & Sreekumar, S. 2017, Current Science, 113, 595, doi: 10.18520/cs/v113/i04/595-598

Robitaille, T. P., Tollerud, E. J., Greenfield, P., et al. 2013, Astronomy & Astrophysics, 558, A33, doi: 10.1051/0004-6361/201322068

Saleem, M., Rana, J., Gayathri, V., et al. 2022, Classical and Quantum Gravity, 39, 025004, doi: 10.1088/1361-6382/ac3b99

Shanmugam, M., Vadawale, S. V., Patel, A. R., et al. 2020, Current Science, 118, 45. https://arxiv.org/abs/1910.09231

Singh, K. P., Tandon, S. N., Agrawal, P. C., et al. 2014, in Space Telescopes and Instrumentation 2014: Ultraviolet to Gamma Ray, ed. T. Takahashi, J.-W. A. den Herder, & M. Bautz, Vol. 9144, 91441S, doi: 10.1117/12.2062667

Tohuvavohu, A., Kennea, J. A., DeLaunay, J., et al. 2020, ApJ, 900, 35, doi: 10.3847/1538-4357/aba94f

Vadawale, S., Purohit, S., Shanmugam, M., et al. 2009, Nuclear Instruments and Methods in Physics Research Section A: Accelerators, Spectrometers, Detectors and Associated Equipment, 598, 485, doi: 10.1016/j.nima.2008.09.036

Vadawale, S., Chattopadhyay, T., Mithun, N., et al. 2018, Nature Astronomy, 2, 50, doi: 10.1038/s41550-017-0293-z

Vadawale, S. V., Chattopadhyay, T., Rao, A. R., et al. 2015, Astronomy & Astrophysics, 578, A73, doi: 10.1051/0004-6361/201525686

Vadawale, S. V., Shanmugam, M., Acharya, Y. B., et al. 2014, Advances in Space Research, 54, 2021, doi: 10.1016/j.asr.2013.06.002

van der Walt, S., Colbert, S. C., & Varoquaux, G. 2011, Computing in Science & Engineering, 13, 22, doi: 10.1109/MCSE.2011.37

van Haarlem, M. P., Wise, M. W., Gunst, A. W., et al. 2013, A&A, 556, A2, doi: 10.1051/0004-6361/201220873

von Kienlin, A., Meegan, C. A., Paciesas, W. S., et al. 2020, ApJ, 893, 46, doi: 10.3847/1538-4357/ab7a18

Watson, D., Hansen, C. J., Selsing, J., et al. 2019, Nature, 574, 497, doi: 10.1038/s41586-019-1676-3

Wei, J., Cordier, B., Antier, S., et al. 2016, arXiv e-prints. https://arxiv.org/abs/1610.06892

Wells, D., Greisen, E., & Harten, R. 1981, Astronomy and Astrophysics Supplement Series, 44, 363

Zhang, D., Li, X., Xiong, S., et al. 2019, Nuclear Instruments and Methods in Physics Research, Section A: Accelerators, Spectrometers, Detectors and Associated Equipment, 921, 8, doi: 10.1016/j.nima.2018.12.032

Zheng, S. 2019, in The Extragalactic Explosive Universe: the New Era of Transient Surveys and Data-Driven Discovery, 63, doi: 10.5281/zenodo.3478126